EXPRESS LETTER

Effect of the mirror force on the collision rate due to energetic electron precipitation: Monte Carlo simulations

Yuto Katoh[1]* , Paul Simon Rosendahl[2,3], Yasunobu Ogawa[4], Yasutaka Hiraki[5] and Hiroyasu Tadokoro[6]

Abstract

We study the effect of the mirror force on the collision rate due to the energetic electron precipitation into the ionosphere. We solve the motion of individual precipitating electrons with the mirror force, where collisions with neutral gas are computed by the Monte Carlo method. By comparing the results with those without the mirror force, we examine the effect of the mirror force on the altitude profile of the ionization rate. First, we carry out simulations of mono-energetic precipitation of 3 keV electrons whose initial pitch angle is 70 degrees at 400 km at $L = 6.45$. We find that the collision rate peaks at around 120 km altitude and that the duration of the collision is scattered in time with a delay of about 5 ms compared with the result without mirror force. Next, we perform mono-energetic precipitation of the different energy and pitch angle ranges. Simulation results demonstrate that larger kinetic energy lowers the altitude profiles of the collision rate, consistent with previous studies. We also find that the upward motion of electrons bounced back from their mirror points results in the upward broadening of the altitude profile of the collision rate. Simulation results for electrons with kinetic energies above 100 keV show that a secondary peak of the collision rate is formed near the mirror point. The formation of the secondary peak can be explained by the stagnation of electrons around the mirror point at 130 km altitude, because the relatively long duration of staying in neutral gas increases the number of collisions. Simulation results show that under the precipitation of electrons in the kinetic energy range larger than tens of keV with the pitch angle close to the loss cone, the maximum collision rate in the altitude range lower than 100 km becomes one order of the magnitude smaller. The results of the present study suggest the importance of the mirror force for the precise modeling of ionospheric response due to the energetic electron precipitation caused by the pitch angle scattering through wave–particle interactions.

Keywords Energetic electron precipitation, Collision rate, Elastic scattering, Numerical simulation
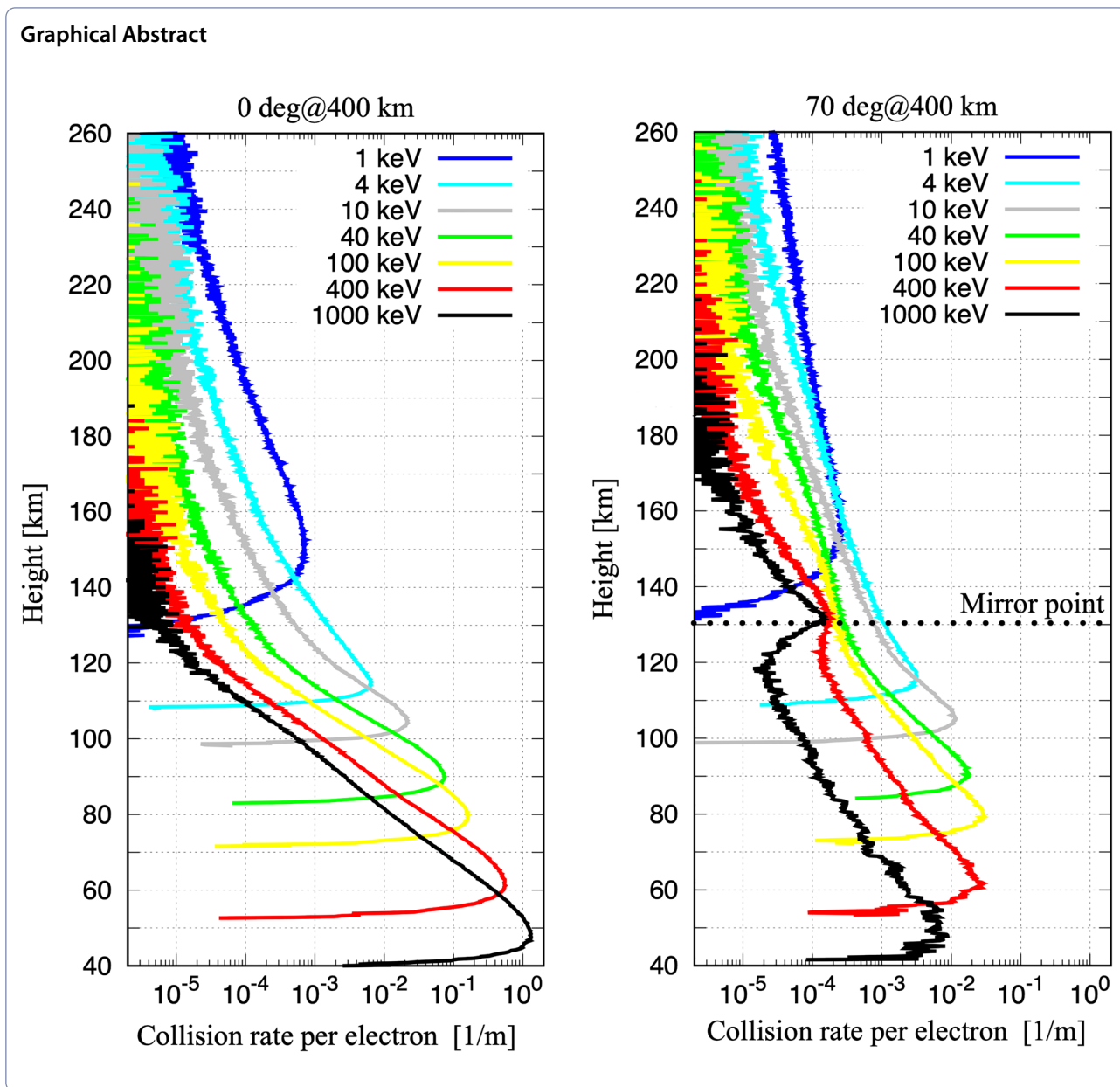
*Correspondence:
Yuto Katoh
yuto.katoh@tohoku.ac.jp
Full list of author information is available at the end of the article

Katoh *et al. Earth, Planets and Space* (2023) 75:117

Page 2 of 11

Graphical Abstract

Main text

Introduction

Energetic electrons precipitating into the ionosphere collide with neutral gas and contribute to various ionospheric phenomena, such as auroral emissions, electron density enhancement, and cosmic noise absorption (e.g., Tao et al. 2020; Oigawa et al. 2021; Tsuda et al. 2021). While the temporal and spatial scales of electron precipitation are controlled by processes occurring in the magnetosphere, the roles of wave–particle interactions have been studied for decades to determine where, when, and how electron precipitation occurs. In this current of the study, it has been widely recognized that whistler-mode waves play important roles in scattering energetic electrons into the loss cone in the magnetosphere as well as the acceleration of radiation belt electrons (e.g., Baker 2021; Martinez-Calderon et al. 2021). Recent progress of the theoretical and simulation studies clarified that nonlinear wave–particle interactions between whistler-mode chorus emissions and energetic electrons are essential in the wave generation process as well as the acceleration/scattering of energetic electrons (Omura et al. 2008, 2009; Katoh et al. 2018; Kitahara

Katoh *et al. Earth, Planets and Space* (2023) 75:117

Page 3 of 11

and Katoh 2019; Omura 2021; Nunn 2021; Foster et al. 2021; Liu et al. 2021). Recent studies suggest that the periodicities of pulsating aurora can be explained by the characteristic time scale of chorus emissions [see Nishimura et al. (2020) and references therein]. The pitch angle scattering of electrons by chorus emissions occurs in the wide energy range from a few keV to higher than hundreds of keV. Electromagnetic ion cyclotron emissions also contribute to the precipitation of relativistic electrons (e.g., Hirai et al. 2018; Grach et al. 2021). Electrons with larger kinetic energy penetrate into lower altitudes (Rees 1963; Miyoshi et al. 2015. Turunen et al. (2009) studied the energetic/relativistic particle precipitation and its effects on the middle/lower atmosphere. A precise understanding of the energetic electron precipitation is crucial to advancing space weather research and operational forecasts (Kusano et al. 2021). The precipitating electrons (> 50 eV) also drive the ion outflow from the ionosphere (Kitamura et al. 2021). While these previous studies revealed the importance of energetic particle precipitation in the ionosphere–magnetosphere coupling system, some of the fundamental processes have not been fully understood and have been treated through a simplifying assumption. One of the processes is the role of the mirror force acting on the precipitating particles. For the quantitative study of the relationship between energetic electron precipitation and ionospheric response, numerical experiments enable us to simulate realistic properties of precipitation and the resultant response occurring in the polar ionosphere.

The collision process between precipitating electrons and neutral gas has been modeled by previous studies (e.g., Lummerzheim et al. 1989). The effect of the mirror force, however, has not been fully included because of the small change in the magnetic field strength in the altitude range of precipitation (Rees 1963). On the other hand, the effect of the mirror force should be significant for electrons having a larger pitch angle close to the loss cone, which should often appear for the electron precipitation caused by the pitch angle scattering through wave–particle interaction in the magnetosphere. Marshall and Bortnik (2018) pointed out the significant effects of the mirror force on the "backscatter" of radiation belt electrons inside the bounce loss cone. The quantitative evaluation of the mirror force on the precipitating electrons is required.

In the present study, we develop a simulation code for the altitude profile of the number of collisions due to the energetic/relativistic electron precipitation. In particular, we focus on the roles of the mirror force acting on precipitating electrons to the altitude profiles of the collision rate. We discuss the energy dependence and the effect of the mirror force on the altitude profile of the collision rate quantitatively.

Model

We compute the motion of energetic particles precipitating along a field line considering the mirror force acting on the particles. We use a cylindrical coordinate system (r, ϕ, z) aligned with the reference magnetic field, where z is defined along the magnetic field line, r is the distance from the axis z, and ϕ is the azimuthal angle from a chosen reference direction defined on the plane perpendicular to the magnetic field. Although the background magnetic field in the polar ionosphere is expressed by the dipole field, we simplify it by a nonuniform cylindrical magnetic field (B_r, B_ϕ, B_z), while we assume that $B_\phi = 0$ and B_r is given by

$$B_r = -\frac{r}{2}\frac{\partial B_z}{\partial z} \tag{1}$$

to satisfy $\nabla \cdot \boldsymbol{B} = 0$ (Katoh and Omura 2006). We consider the spatial gradient of the magnetic field intensity along the z axis following the dipole magnetic field with the dipole moment 8.05×10^{22} A m^2. The equation of the motion of a charged particle in the background magnetic field $\boldsymbol{B}$ including the relativistic effect is given by

$$\frac{\mathrm{d}(m_0\gamma\boldsymbol{v})}{\mathrm{d}t} = \frac{d\boldsymbol{p}}{dt} = q\boldsymbol{v} \times \boldsymbol{B}, \tag{2}$$

where $\boldsymbol{p}$, q and m_0 represent the momentum, charge, and the rest mass of a particle, respectively, and γ is the Lorentz factor. Here, we ignore the electric field in (2) and discuss the effect of the electric field in the Results and Discussions section. Noting that electrons gyrating around the reference magnetic field at the distance of the Larmor radius r_L see B_r given by (1), we obtain the parallel component of (2) as

$$\frac{dp_\parallel}{dt} = qv_\perp B_r = -|q|v_\perp\frac{r_L}{2}\frac{\partial B_z}{\partial z}, \tag{3}$$

where $v_\perp$ is the velocity component perpendicular to the background magnetic field. We also employ the energy conservation law:

$$p_0^2 = p_\parallel^2 + p_\perp^2 \tag{4}$$

where p_0 is the absolute value of the momentum of a charged particle. The set of Eqs. (3) and (4) enables us to compute the variation of the pitch angle due to the mirror force during the precipitation of a charged particle.

We also employ a module computing the altitude distribution of collisions between neutral gas and precipitating energetic electrons in the polar ionosphere. We

Katoh *et al. Earth, Planets and Space* (2023) 75:117

Page 4 of 11

use a Monte Carlo method to derive the collision rate by the precipitating electrons, as has been used in previous studies (e.g., Solomon 2001; Hiraki and Tao 2008). Only elastic collision and ionization cross section are considered, because these two processes are dominant in the energy range higher than 100 eV (cf. Hiraki and Tao 2008; Tawara et al. 1990). The probability of a collision between energetic electrons and neutral gas during the time interval Δt is given by Cashwell and Everett (1959)

$$P_i = 1 - \exp\{-N(z_i)\sigma_{tot}(\varepsilon_i)v_i\Delta t\}, \tag{5}$$

where P_i is the probability of a collision between the i-th electron and neutral gas, $N(z_i)$ is the total atmospheric gas density at an altitude z_i of i-th electron, $\sigma_{tot}(\varepsilon_i)$ is the sum of the collision cross sections for the kinetic energy ε_i, and v_i is the velocity of i-th electron. The MSIS-E-90 model (Hedin 1991) is used for the altitude distribution of neutrals (O, N_2, O_2, and He) at $L = 6.45$ (Fig. 1a), corresponding to Tromsø, Norway. We assumed the local time 00:00 of 1 January 2018 with the input parameters of the solar and geomagnetic activities taken from the real

database; F10.7 was 66.8 SFU and Ap index was 12 on the assumed date. We refer to ionization cross sections by the Binary Encounter Bethe model (Kim and Rudd 1994) with parameters provided by NIST (https://www.nist.gov/pml). Elastic scattering cross section and its pitch angle dependence are given by Lummerzheim (1987) and Lummerzheim et al. (1989), respectively. According to Hiraki and Tao (2008), since the Monte Carlo method used in the present study allows only one collision per electron in Δt, we change Δt if necessary to meet $P_i < 0.1$ with the probability of a multiple collision being less than 1% in every time step. The Δt ranges from 0.5 to 1000 Ω_{e0}^{-1}, where Ω_{e0} is the gyrofrequency at 400 km, due to the significant difference in the altitude profile of the neutral gas density. The production of secondary electrons is not considered, because we focus on the effect of the mirror force on the collision rate but should be taken into account if we extend our model to the computation of ionization rate profiles.

By combining the developed modules, we study the time scale and intensity of the collision rate due to the
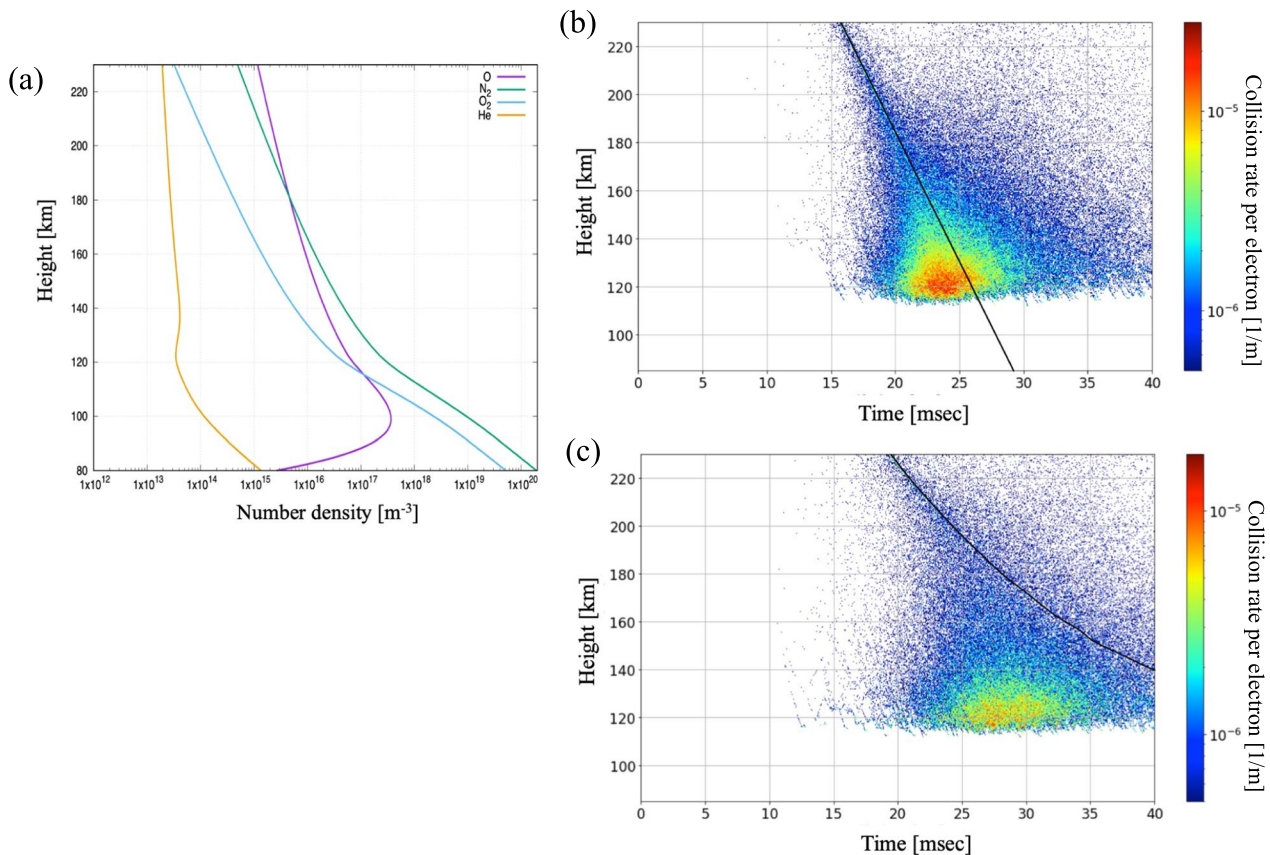

Fig. 1 **a** Altitude profiles of neutral atoms and molecules (O, N_2, O_2, and He) obtained by the MSISE-90 model at $L = 6.45$. **b** Time history of the altitude profile of collision rate per electron obtained by the simulation without mirror force acting on electrons. **c** Simulation results with mirror force acting on electrons. 3 keV electrons whose initial pitch angle of 70 degrees at 400 km are assumed in both **b** and **c**

Katoh *et al. Earth, Planets and Space*   (2023) 75:117

Page 5 of 11

energetic electron precipitation. The flow of the simulation is described as follows:

Step 1. The i-th electron is placed at 400 km with the momentum vector $(p_\parallel, p_\perp)$, corresponding to the assumed initial kinetic energy and pitch angle.

Step 2. The position z_i of the i-th electron is updated by computing $z_i + v_\parallel \Delta t$, where $v_\parallel$ is the parallel component of the velocity vector.

Step 3. Evaluation of the probability of the collision by (5) using the kinetic energy of the i-th electron. We generate a random number between 0 and 1 and determine that a collision occurred for the i-th electron when the obtained number is less than P_i. If a collision occurred, we then evaluate the probabilities of elastic collision and ionization; we generate another random number to determine that ionization or elastic collision occurred or not, by referring to the collision cross sections of the assumed neutral species. If ionization occurred, we evaluate the collision pair and subtract the corresponding ionization energy from the i-th electron. If the elastic collision occurred, we compute the scattering angle due to the collision using the screened (Rutherford formula Lummerzheim et al. 1989) and then change the pitch angle of the i-th electron.

Step 4. We update the momentum vector $(p_\parallel, p_\perp)$ by referring to the background magnetic field vector at the updated position z_i. This step will be skipped if we do not consider the mirror force acting on the i-th electron.

Step 5. We continue Step 2–4 until the kinetic energy of the i-th electron becomes less than the ionization energy. We also terminate the computation if the i-th electron reached the ground or 400 km altitude during its bounce motion. After finishing the computation of the ith electron, we return to Step 1 for the next $(i+1)$-th electron. We compute 10,000 electrons in total.

We carry out the simulation for a wide energy and pitch angle ranges, focusing on the effect of the mirror force on the motion of precipitating electrons into the polar ionosphere.

Results and discussion

First, we carry out simulations of mono-energetic precipitation of 3 keV electrons whose initial pitch angle is 70 degrees at 400 km at $L = 6.45$. In the dipole field, the mirror point is located at 130 km altitude for a particle whose pitch angle is 70 degrees at 400 km. Figure 1b, c shows the time evolution of the altitude profile of the collision rate per electron obtained by the simulations without (Fig. 1b) and with (Fig. 1c) mirror force acting on electrons, where the collision rate per electron is defined as the number of collisions expected to occur in a unit volume per incident unit electron flux cf. Rees 1963; We counted the number of collisions that occurred by incident electrons at each altitude grid and divided it by the grid width and the number of computed electrons to obtain the number of collisions per unit length of altitude by one incident electron. By this definition, we can obtain the number of collisions in a unit volume per unit time $[\text{m}^{-3}\,\text{s}^{-1}]$ by multiplying the computed collision rate $[\text{m}^{-1}]$ with an incident electron flux $[\text{m}^{-2}\,\text{s}^{-1}]$. The black solid line in Fig. 1b, c indicates the trajectory of an electron of the assumed initial kinetic energy and pitch angle without collision. Because of the scattering due to elastic collisions, trajectories of precipitating electrons deviate from the black solid line. The increase in the number density of the neutral gases results in the peak of the collision rate at around 120 km altitude. The effect of the mirror force changes the time evolution of the collision rate, as shown in Fig. 1c; at an altitude of 120 km, the duration of the collision is scattered in time and the peak of the collision rate is delayed about 5 ms compared with the result without mirror force (Fig. 1b).

Next, we carry out simulations of mono-energetic precipitation of the different energy and pitch angle ranges with the mirror force. Figure 2 shows the time histories of the altitude profiles of the collision rate per electron obtained by a series of simulations. The initial kinetic energy of (a, d, g) 1 keV, (b, e, h) 3 keV, and (c, f, i) 10 keV and the initial pitch angle of (a–c) 0 degree, (d–f) 30 degree, and (g–i) 60 degree are assumed at 400 km. Figure 2 clearly demonstrates that larger kinetic energy lowers the altitude profiles of the collision rate. Figure 2 also indicates that a larger pitch angle delays the evolution of the collision rate. The delay can be explained by a smaller initial $v_\parallel$ for the larger initial pitch angle and by the increase of the pitch angle during the precipitation due to the mirror force. We note in the time interval after the peak of the collision rate, the V-shaped upward spread of the collision rate appears in all panels, especially in the smaller initial pitch angle (Fig. 2a–f). The upward spread is caused by the "backscattered" electrons moving upward (Marshall and Bortnik 2018); these electrons underwent collisions during the precipitation but survived and bounced back from the mirror point.

By integrating the evolution of the collision rate in time, we obtain the altitude profiles of the collision rate per electron. Figure 3 shows the altitude profiles of the collision rate per electron for the cases of mono-energetic precipitation of 1, 4, 10, and 40 keV electrons, whose initial pitch angle is (a) 0 and (b) 70 degrees, at an altitude
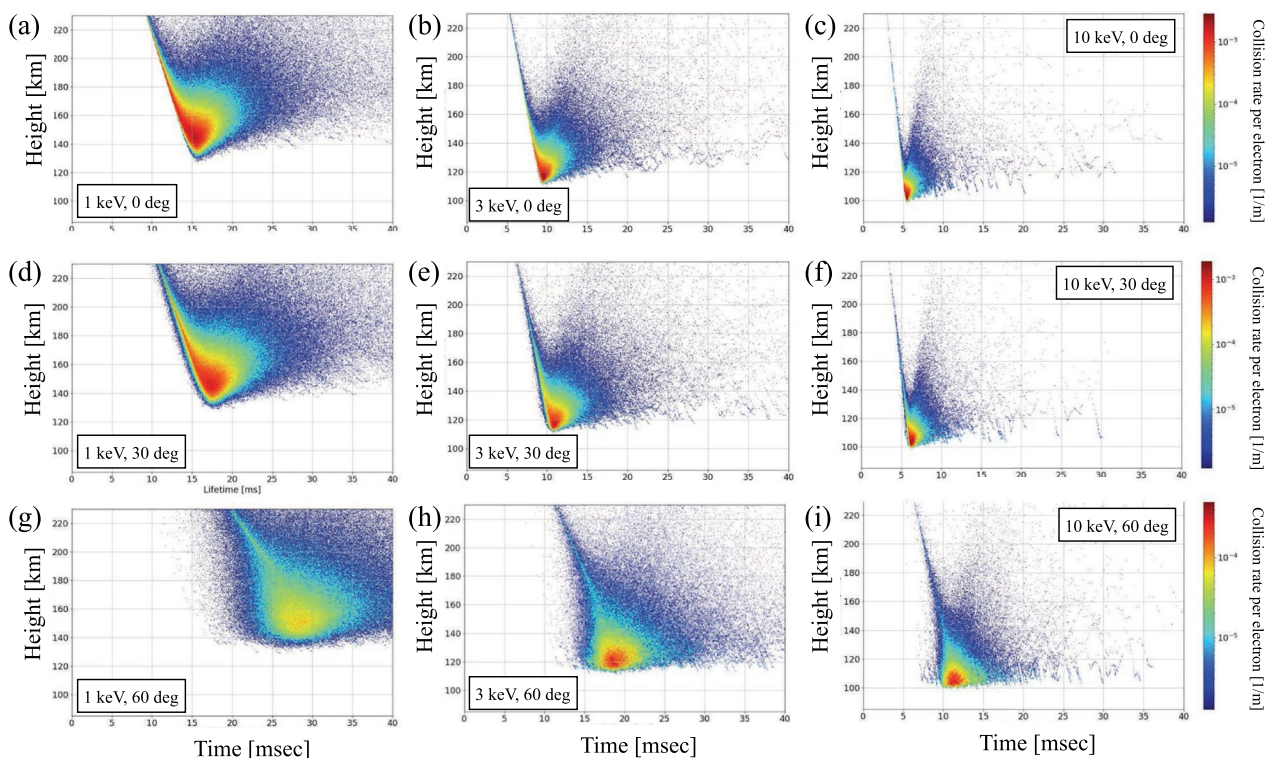
Fig. 2 Time histories of the altitude profiles of the collision rate per electron obtained by a series of simulations with mirror force. The initial kinetic energy of (**a**, **d**, **g**) 1 keV, (**b**, **e**, **h**) 3 keV, and (**c**, **f**, **i**) 10 keV and the initial pitch angle of (**a**–**c**) 0 degree, (**d**–**f**) 30 degree, and (**g**–**i**) 60 degree are assumed at 400 km

of 400 km. We note that the stopping height reproduced in Fig. 3a, b is lower than those reported in Rees (1963), because the number density of neutrals was lower than those used in Rees (1963). Since previous studies also reported penetration of tens of keV electrons below 90 km altitude (Solomon 2001; Turunen et al. 2009), we consider that the ionization profiles obtained by our simulation code are consistent with previously reported results. Solid and dotted lines show the simulation results with and without mirror force, respectively. In Fig. 3a, the solid and dotted lines are almost overlapped, indicating that the effect of the mirror force is negligible for the 0 degrees initial pitch agnel. The deviation of the solid line from the dotted line is evident in Fig. 3b. While the altitude of the peak of the collision rate is almost unchanged for all energy ranges, the maximum collision rate becomes about one-half of those without mirror force. In addition, the upward spread of the altitude profiles is identified in the results of 40 keV electrons; the collision rate per electron obtained with mirror force becomes larger than those obtained without mirror force at an altitude higher than the mirror point. As we found in Fig. 2, backscattered electrons due to the mirror force are responsible for the upward shift of the collision rate.

Figure 3c, d show the total number of collisions that occurred through the mono-energetic precipitation of 1 keV (Fig. 3c) and 40 keV (Fig. 3d) electrons as a function of the initial pitch angle at 400 km; the total number of collisions is normalized by that of the initial pitch angle of 0 degrees and is shown in percentage. The simulation results with and without mirror force are shown in blue and red solid lines, respectively. The difference between the blue and red lines is not evident in the smaller pitch angle ranges, as shown in Fig. 3a, but becomes gradually significant in the pitch angle range larger than 45 degrees. Noting that the mirror point is located at 100 km for electrons having 69 degrees pitch angle at 400 km, 40 keV electrons having a pitch angle larger than 75 degrees do not collide with neutral gases due to both mirror force and small collision cross sections. For 1 keV electrons, the significance of the mirror force is the same as 40 keV electrons but the relatively large cross section results in a certain number of collisions occurring in the pitch angle range larger than 75 degrees. Figure 3c, d suggest that the energy-dependent collision cross section is responsible for the relatively weak effect of the mirror force in the lower energy range in Fig. 3b; the larger collision cross section of the lower energy range weakens the effect of
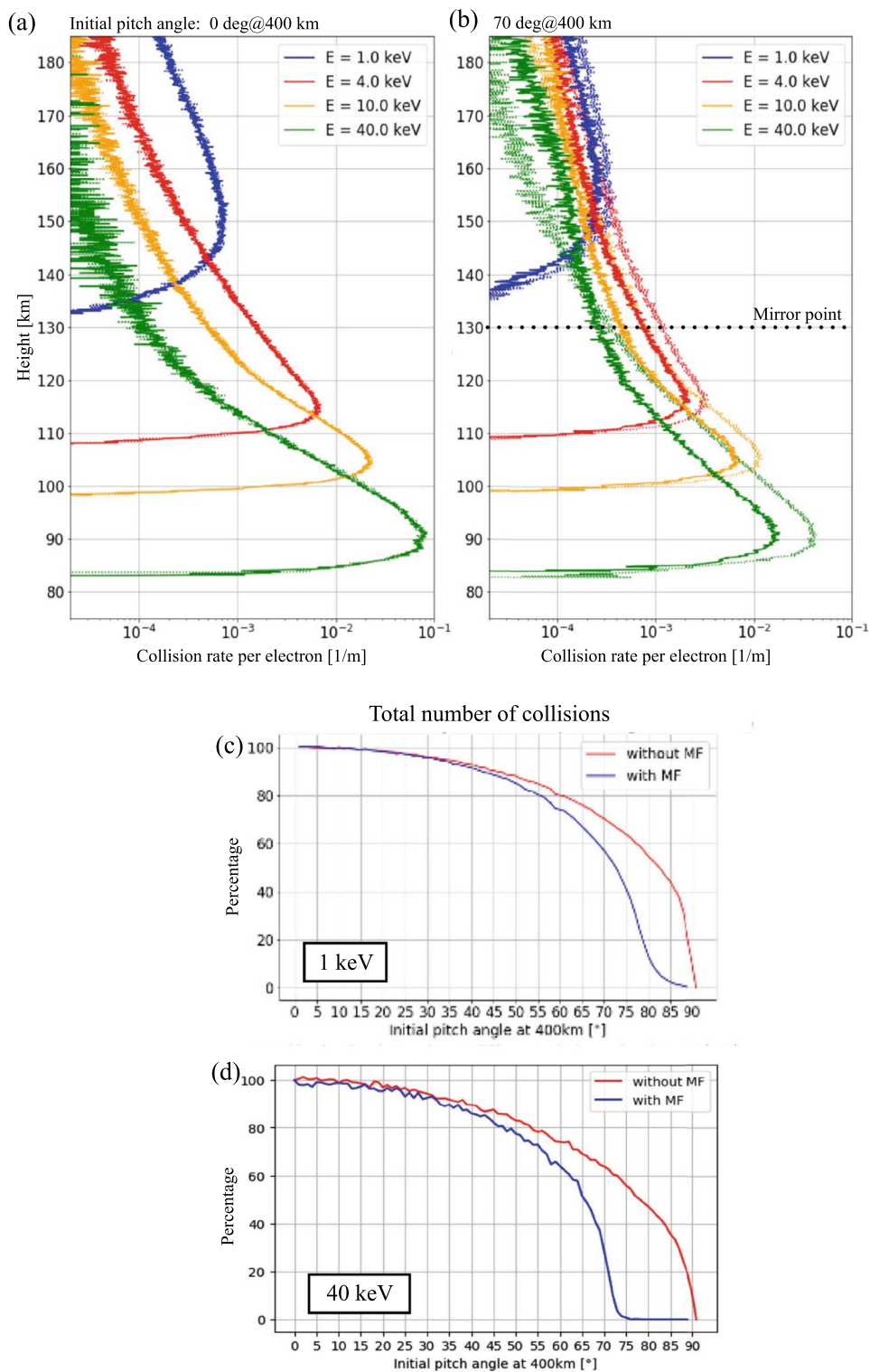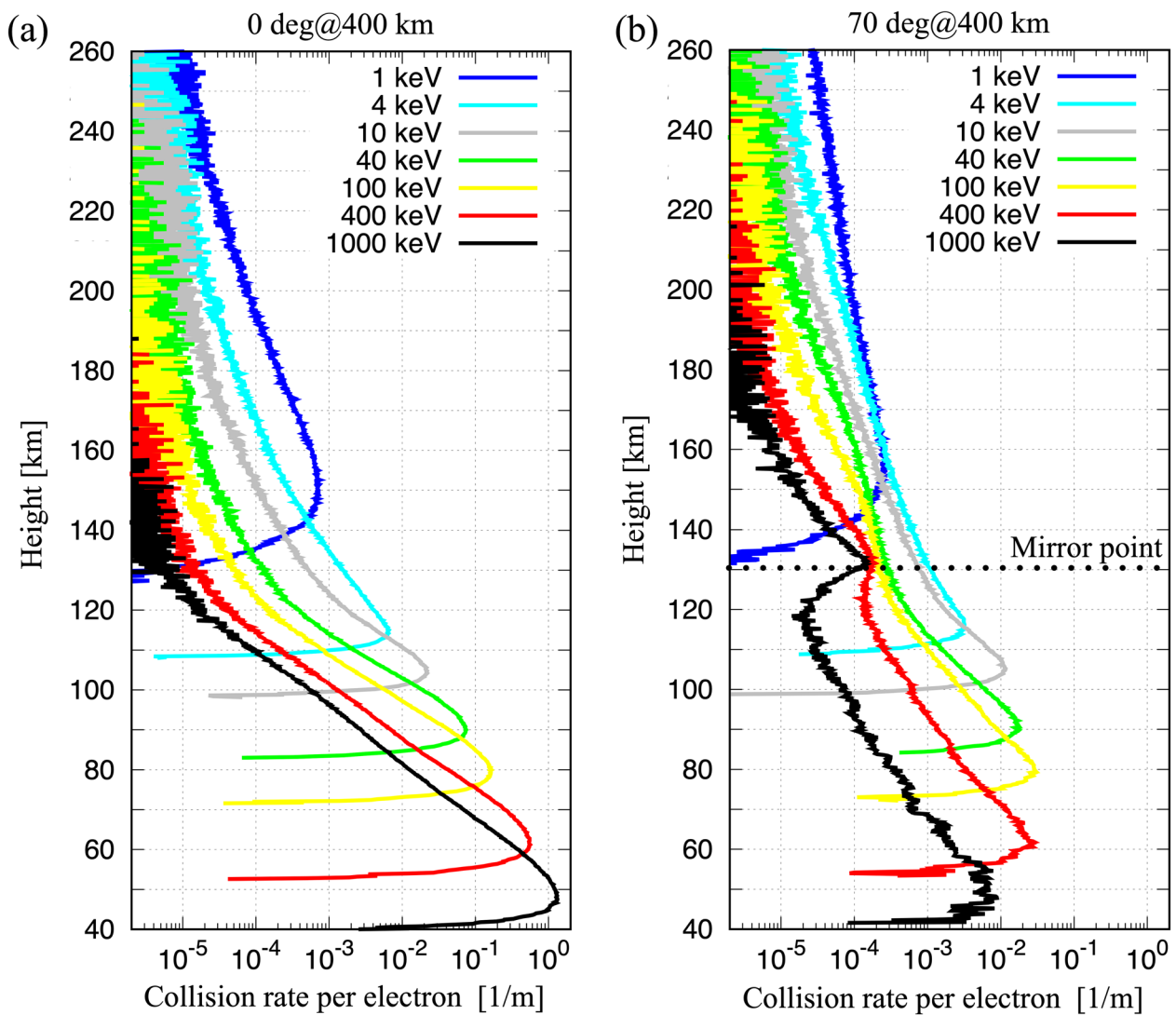
Fig. 3 a, **b** Altitude profiles of the collision rate per electron for the cases of mono-energetic precipitation of 1, 4, 10, and 40 keV electrons, whose initial pitch angle is (**a**) 0 and (**b**) 70 degrees, at an altitude of 400 km. Solid and dotted lines show the simulation results with and without mirror force, respectively. **c**, **d** Total number of collisions occurred through the mono-energetic precipitation of (**c**) 1 keV and (**d**) 40 keV electrons as a function of the initial pitch angle at 400 km. The simulation results with and without mirror force are shown in blue and red solid lines, respectively

Fig. 4 Altitude profiles of the collision rate per electron for the cases of mono-energetic precipitation of 1, 4, 10, 40, 100, 400, and 1000 keV electrons, whose initial pitch angle is (**a**) 0 degrees and (**b**) 70 degrees at an altitude of 400 km, obtained by the simulations with mirror force

the mirror force, because most of the electrons are lost before reaching their mirror point.

Finally, we extend the kinetic energy range from 1 to 1000 keV. Figure 4 shows the altitude profiles of the collision rate per electron obtained by the simulation results, assuming the initial pitch angle of 0 degrees (Fig. 4a) and 70 degrees (Fig. 4b) at 400 km. The larger kinetic energy lowers the peak altitude of the collision rate per electron, as expected from the energy-dependent collision cross section (Rees 1963; Turunen et al. 2009). For the case of the initial pitch angle of 0 degrees at 400 km, we confirmed that the altitude profiles of the collision rate per electron were almost unchanged with and without mirror force. On the other hand, the effect of the mirror

force is significant in the case of 70 degrees pitch angle, as shown in Fig. 3. We find the decrease in the maximum collision rate and upward spread of the altitude profiles in all energy range assumed, while the difference between Fig. 4a, b becomes significant in the higher energy range. In the energy range larger than 100 keV, we find the formation of the second peak around the mirror point. The amount of the second peak is 2 orders of magnitude smaller than that of the first peak at the lower altitude. Stagnation around the mirror point makes the relatively long duration staying of energetic electrons in neutral gas, and it results in an increase of the collision rate around the mirror point, against the relatively smaller collision cross section in the higher energy range.

Katoh *et al. Earth, Planets and Space*   (2023) 75:117

Page 9 of 11

Figure 4 reveals that the effect of the mirror force acting on precipitating electrons should be important to the ionization rate in the lower ionosphere caused by electrons in the higher energy range. Conventional models computed the altitude profiles of electron density in the ionosphere using the ionization rate derived without considering the mirror force (e.g., Solomon 2001). However, the pitch angle dependence revealed by the present study (Fig. 4) suggests the importance of the mirror force; the collision rate in the altitude range lower than 100 km becomes one order of magnitude smaller if electrons in the kinetic energy range larger than tens of keV precipitate with the pitch angle close to the loss cone. Electrons near the loss cone should be commonly observed in the cases of energetic electron precipitation due to the pitch angle scattering by plasma waves. The development of a model for the ionization rate considering the mirror force is important for the precise modeling of ionospheric response due to the energetic electron precipitation.

Figure 5 illustrates the role of the mirror force on the motion of precipitating electrons and the scattering by collisions. Figure 5a, b show the cases without and with mirror force, respectively. The horizontal magnitude of each arrow in the figure actually indicates the component of the gyro-motion of electrons. In Fig. 5a, the scattered electrons change their velocity vectors due to the scattering, but the motion after the scattering is straight until the next collision. In Fig. 5b, on the other hand, the velocity vectors of precipitating electrons are forced to be upward due to the presence of the mirror force, resulting in the upward broadening of the collision rate and the formation of the second peak due to the enhanced backscattered electrons.
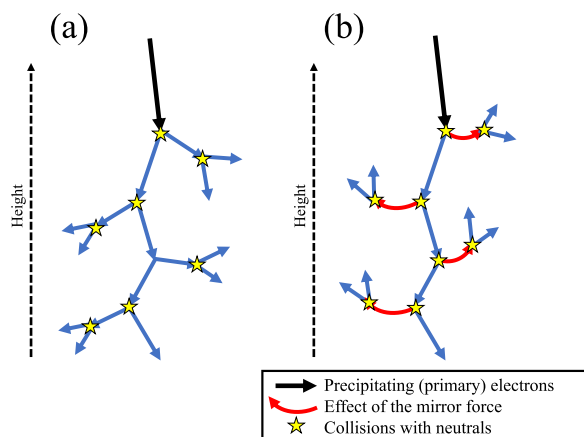

Fig. 5 Illustration showing the relation between precipitating electrons, mirror force, and collisions with neutrals. The cases (**a**) without and (**b**) with mirror force are shown

In the present study, we ignored the effect of the electric field on the motion of electrons, as given by (2). We ignored the perpendicular electric field corresponding to the convection electric field, because the time scale of the simulation is tens of msec, and therefore, the effect of the convection motion can be negligible in the present results. In addition, since we focus on the electron precipitation due to the pitch angle scattering by magnetospheric plasma waves typically observed in the sub-auroral latitude, we ignored the field-aligned electric field. In the auroral zone related to discrete aurora, on the other hand, we expect significant field-aligned acceleration resulting in the enhancement of the electron flux in the small pitch angle range. Our results showed that the effect of the mirror force is relatively weaker in the smaller pitch angle range (Fig. 3), and therefore, the conventional approach simplifying the pitch angle dependence would be reasonable in the auroral zone.

We used the spatially one-dimensional profiles of the neutral composition based on the MSIS-E-90 atmosphere model, so the horizontally uniform atmosphere was used. Since the time scale of the precipitation is tens of msec, the horizontal motion of energetic electrons can be negligible. Although the altitude profiles of the neutral composition should significantly affect the altitude profiles of the ionization rate, the effect of the mirror force investigated in the present study should work likewise.

Summary

The effect of the mirror force has not been fully included in the previous studies of collision between precipitating electrons and neutral gas because of the small change in the magnetic field strength at the ionospheric altitude and the significant pitch angle scattering through collisions. However, in the present study, we showed that it is not necessarily the case for electrons having a large pitch angle close to the loss cone.

We developed a simulation code for the motion of energetic electrons with the mirror force acting on the precipitating electrons, which enables us to solve the variation of the pitch angle of the electrons during their precipitation. We also employ a module computing the altitude distribution of the collision rate by precipitating energetic electrons in the polar ionosphere. We use the Monte Carlo method to derive the collision rate by the precipitating electrons, as has been used in previous studies (e.g., Hiraki and Tao 2008). By combining the developed modules, we studied the time scale and intensity of the collision rate due to the energetic electron precipitation.

The simulation results showed that the influence of the mirror force on the altitude profile of collision rate is significant for electrons with a high initial pitch

Katoh *et al. Earth, Planets and Space* (2023) 75:117

Page 10 of 11

angle, corresponding to the pitch angle close to the loss cone. The effect of the mirror force results in the broadening of the altitude profile of the collision rate upward due to the reflection of mirroring electrons. The simulation results with energetic electrons whose kinetic energy is larger than 100 keV showed the formation of the secondary peak around the mirror point in the altitude profile of the collision rate. The formation of the secondary peak can be explained by the stagnation of electrons around the mirror point. The relatively long duration staying in neutral gas results in the increase of the collision rate around the mirror point, against the smaller collision cross section in the higher energy range.

We revealed that the pitch angle dependence of the collision rate due to the mirror force alters the maximum collision rate in the altitude range lower than 100 km one order of magnitude smaller if electrons in the kinetic energy range larger than tens of keV precipitate with the pitch angle close to the loss cone. The results of the present study emphasize the importance of the mirror force for the precise modeling of ionospheric response due to the energetic electron precipitation. The development of a model for the ionization rate considering the mirror force is an important future study.

Availability of data and materials
The data sets used and/or analysed during the current study are available from the corresponding author on reasonable request.

Declarations

Ethics approval and consent to participate
Not applicable.

Consent for publication
Not applicable.

Competing interests
The authors declare that they have no competing interests.

Author details
[1]Graduate School of Science, Tohoku University, Sendai, Japan. [2]Faculty of Physics and Astronomy, Heidelberg University, Heidelberg, Germany. [3]Faculty of Science, Tohoku University, Sendai, Japan. [4]National Institute of Polar Research, Tachikawa, Japan. [5]Advanced Knowledge Laboratory, Inc., Shinjuku, Japan. [6]Chiba Keizai University, Chiba, Japan.

References
Baker DN (2021) Wave–particle interaction effects in the Van Allen belts. Earth Planets Space 73:189. https://doi.org/10.1186/s40623-021-01508-y

Cashwell ED, Everett CJ (1959) A practical manual of the monte carlo method for random walk problems. Pergamon, New York

Foster JC, Erickson PJ, Omura Y (2021) Subpacket structure in strong VLF chorus rising tones: characteristics and consequences for relativistic electron acceleration. Earth Planets Space 73:140. https://doi.org/10.1186/s40623-021-01467-4

Grach VS, Demekhov AG, Larchenko AV (2021) Resonant interaction of relativistic electrons with realistic electromagnetic ion–cyclotron wave packets. Earth Planets Space. https://doi.org/10.1186/s40623-021-01453-w

Hedin AE (1991) Extension of the MSIS thermosphere model into the middle and lower atmosphere. J Geophys Res 96:1159–1172. https://doi.org/10.1029/90JA02125

Hirai A, Tsuchiya F, Obara T, Kasaba Y, Katoh Y, Misawa H et al (2018) Temporal and spatial correspondence of Pc1/EMIC waves and relativistic electron precipitations observed with ground-based multi-instruments on 27 March 2017. Geophys Res Lett. https://doi.org/10.1029/2018GL080126

Hiraki Y, Tao C (2008) Parameterization of ionization rate by auroral electron precipitation in Jupiter. Ann Geophys 26:77–86. https://doi.org/10.5194/angeo-26-77-2008

Katoh Y, Omura Y (2006) A study of generation mechanism of VLF triggered emission by self-consistent particle code. J Geophys Res 111:A12207. https://doi.org/10.1029/2006JA011704

Katoh Y, Omura Y, Miyake Y, Usui H, Nakashima H (2018) Dependence of generation of whistler mode chorus emissions on the temperature anisotropy and density of energetic electrons in the earth's inner magnetosphere. J Geophys Res Space Phys 123:1165–1177. https://doi.org/10.1002/2017JA024801

Kim Y-K, Rudd ME (1994) Binary-encounter-dipole model for electron-impact ionization. Phys Rev A 50(5):3954–3967. https://doi.org/10.1103/PhysRevA.50.3954

Kitahara M, Katoh Y (2019) Anomalous trapping of low pitch angle electrons by coherent whistler mode waves. J Geophys Res Space Phys 124:5568–5583. https://doi.org/10.1029/2019JA026493

Kitamura N, Seki K, Keika K et al (2021) On the relationship between energy input to the ionosphere and the ion outflow flux under different solar zenith angles. Earth Planets Space 73:202. https://doi.org/10.1186/s40623-021-01532-y

Kusano K, Ichimoto K, Ishii M et al (2021) PSTEP: project for solar–terrestrial environment prediction. Earth Planets Space 73:159. https://doi.org/10.1186/s40623-021-01486-1

Liu Y, Omura Y, Hikishima M (2021) Simulation study on parametric dependence of whistler-mode hiss generation in the plasmasphere. Earth Planets Space 73:230. https://doi.org/10.1186/s40623-021-01554-6

Lummerzheim D, Rees MH, Anderson HR (1989) Angular dependent transport of auroral electrons in the upper atmosphere. Planet Space Sci 37:109–129. https://doi.org/10.1016/0032-0633(89)90074-3

Lummerzheim, D. (1987) Electron transport and optical emissions, in the aurora, Ph. D thesis, Univ. Alaska, Fairbanks.

Katoh *et al. Earth, Planets and Space*   *(2023) 75:117*

Page 11 of 11

Marshall RA, Bortnik J (2018) Pitch angle dependence of energetic electron precipitation: energy deposition, backscatter, and the bounce loss cone. J Geophys Res Space Phys 123:2412–2423. https://doi.org/10.1002/2017JA024873

Martinez-Calderon C, Manninen JK, Manninen JT et al (2021) A review of unusual VLF bursty-patches observed in Northern Finland for earth, planets and space. Earth Planets Space 73:191. https://doi.org/10.1186/s40623-021-01516-y

Miyoshi Y et al (2015) Energetic electron precipitation associated with pulsating aurora: EISCAT and Van Allen probe observations. J Geophys Res Space Phys 120:2754–2766. https://doi.org/10.1002/2014JA020690

Nishimura Y, Lessard MR, Katoh Y et al (2020) Diffuse and pulsating aurora. Space Sci Rev 216:4. https://doi.org/10.1007/s11214-019-0629-3

Nunn D (2021) The numerical simulation of the generation of lower-band VLF chorus using a quasi-broadband Vlasov hybrid simulation code. Earth Planets Space 73:222. https://doi.org/10.1186/s40623-021-01549-3

Oigawa T, Shinagawa H, Taguchi S (2021) Time-dependent responses of the neutral mass density to fixed magnetospheric energy inputs into the cusp region in the thermosphere during a period of large IMF BY: a high-resolution two-dimensional local modeling. Earth Planets Space 73:201. https://doi.org/10.1186/s40623-021-01535-9

Omura Y (2021) Nonlinear wave growth theory of whistler-mode chorus and hiss emissions in the magnetosphere. Earth Planets Space 73:95. https://doi.org/10.1186/s40623-021-01380-w

Omura Y, Katoh Y, Summers D (2008) Theory and simulation of the generation of whistler-mode chorus. J Geophys Res 113:A04223. https://doi.org/10.1029/2007JA012622

Omura Y, Hikishima M, Katoh Y, Summers D, Yagitani S (2009) Nonlinear mechanisms of lower-band and upper-band VLF chorus emissions in the magnetosphere. J Geophys Res 114:A07217. https://doi.org/10.1029/2009JA014206

Rees MH (1963) Auroral ionization and excitation by incident energetic electrons. Planet Space Sci 11:1209–1218. https://doi.org/10.1016/0032-0633(63)90252-6

Solomon SC (2001) Auroral particle transport using Monte Carlo and hybrid methods. J Geophys Res 106(A1):107–116. https://doi.org/10.1029/2000JA002011

Tao C, Jin H, Miyoshi Y et al (2020) Numerical forecast of the upper atmosphere and ionosphere using GAIA. Earth Planets Space 72:178. https://doi.org/10.1186/s40623-020-01307-x

Tawara H, Itikawa Y, Nishimura H, Yoshino M (1990) Cross sections and related data for electron collisions with hydrogen molecules and molecular ions. J Phys Chem Ref Data 19:3617–3636. https://doi.org/10.1063/1.555856

Tsuda TT, Tanaka YM, Tozu R et al (2021) Relationship between Na layer and CNA variations observed at Syowa, Antarctic. Earth Planets Space 73:7. https://doi.org/10.1186/s40623-020-01335-7

Turunen E et al (2009) Impact of different energies of precipitating particles on NO_x generation in the middle and upper atmosphere during geomagnetic storms. J Atmos Sol Terr Phys 71:1176–1189. https://doi.org/10.1016/j.jastp.2008.07.005

Publisher's Note